

Peter Vorobieff
From ideal fluid flow to understanding lift and drag on wings

These notes are mostly based on the way the subjects of interest are presented in *Fundamental Mechanics of Fluids* by I.G. Currie, Professor Emeritus of Mechanical Engineering at the University of Toronto, to whom I owe a debt of gratitude. The reader would benefit from some prior knowledge of differential equations and complex variable theory; no other specialized skills are required. The notes are not a replacement for the lecture materials, but rather a supplement to them. It is also inevitable that some readers will likely find some topics here explained in too much or too little detail. There is also some deliberate overlap between these notes and those from Professor Nitzche's class, so that the narrative herein can be used both in combination with them or as a standalone document.

A few remarks must be made on notation. In some of the equations here, vector and scalar quantities are used together. Vector quantities (comprised of two or three components, depending on the dimensionality of the problem) are represented by bold letters.

1. Introduction of ideal-fluid flow

What is referred to as ideal fluid here is to some extent the same substance that the scientists in the XVIIIth century considered as just “fluid” - a woefully imprecise, yet useful mathematical approximation of the actual liquids (and gases) that flow in rivers, pour out of bottles, fill our lungs, and so on. The same approximation also (to an extent) works for plasma. The main assumptions that differentiate the ideal fluid from the real thing are that **ideal fluid is inviscid and incompressible**.



Leonhard Euler (1707-1783).

Portrait by Johann Georg Brucker (1756)

“To those who ask what the infinitely small quantity in mathematics is, we answer that it is actually zero. Hence there are not so many mysteries hidden in this concept as they are usually believed to be.”

Inviscid means that viscous dissipation in the medium is negligible. That assumption also leads to the possibility of solving a reduced system of conservation equations, where mass and momentum conservation laws uncouple from the energy equation.

Incompressible means that the density ρ (mass-to-volume ratio) remains constant any infinitesimal volume that moves with the flow. An important subcase of incompressible flow we will mostly deal with is $\rho = \text{const}$ (which means that density is not a variable we have to solve for), although it may be possible to have an incompressible flow where density is not constant (for example, a stably stratified shear flow).

In some cases, these assumptions are pretty reasonable when dealing with real-world problems. It is also noteworthy that ideal fluid can be elegantly described and decently understood mathematically, which, unfortunately, cannot be said for the real fluid. The governing equations for ideal fluid are quite appropriately known as Euler's equations, because Leonhard Euler derived them and published the work in 1757, when he worked at the Berlin Academy, on a 25-year break from

the Russian Imperial Academy of Sciences. These equations (in vector form) are:

$$\begin{aligned}\nabla \cdot \mathbf{u} &= 0 \\ \frac{\partial \mathbf{u}}{\partial t} + (\mathbf{u} \cdot \nabla) \mathbf{u} &= -\frac{1}{\rho} \nabla p + \mathbf{f}\end{aligned}\quad (1.1)$$

The first one is referred to as the **continuity equation** (it follows from the mass conservation law based on the assumption of incompressibility), the second is the momentum equation. Here \mathbf{u} is the velocity vector, ∇ is the differential operator known as del (or nabla), \cdot represents a scalar product of two vectors, t is time, ρ is fluid density, p is pressure, and \mathbf{f} represents the force per mass.

Both equations (1.1) can be derived from general conservation considerations for momentum and energy for a small fluid volume in Cartesian coordinates. The physical meaning of the mass conservation equation is that the volume containing the same amount of fluid molecules remains the same. The momentum equation (strictly speaking, it's one vector equation or three scalar ones) relates the change in momentum of the fluid volume (as a combination of temporal $\partial/\partial t$ and convective $(\mathbf{u} \cdot \nabla)$ derivatives) to the work of pressure and mass forces (right side of equation). Here we will not bother with a formal derivation.

To go from vector notation in (1.1) to components, we must examine the components of individual vectors, taking into account that we have both space- and time-dependent vector quantities (fields) and vector differential operators. Consider, for example, the quantity $\nabla \cdot \mathbf{u}$, which represents a differential operator acting upon a field. If the operator ∇ is applied to a function f defined on a one-dimensional domain (x), it simply produces its derivative (as defined in calculus for a function of a single variable: $\nabla f = df/dx$). Now consider the three-dimensional case, where the velocity \mathbf{u} is a vector comprised of three components:

$$\mathbf{u} = (u, v, w) = \begin{bmatrix} u(x, y, z, t) \\ v(x, y, z, t) \\ w(x, y, z, t) \end{bmatrix}$$

By analogy with the one-dimensional case (x), the three-dimensional (x, y, z) form of the operator ∇ becomes

$$\nabla = \left(\frac{\partial}{\partial x}, \frac{\partial}{\partial y}, \frac{\partial}{\partial z} \right),$$

where the ordinary derivative (symbol d) is replaced with the partial derivative (symbol ∂), to denote dealing with multiple variables. Finally, to obtain the component form from the vector form, we must formally apply the scalar product to $\nabla \cdot \mathbf{u}$, using the same rules we would to obtain the scalar product of two ordinary vectors:

$$\nabla \cdot \mathbf{u} = \left(\frac{\partial}{\partial x}, \frac{\partial}{\partial y}, \frac{\partial}{\partial z} \right) \cdot (u, v, w) = \frac{\partial u}{\partial x} + \frac{\partial v}{\partial y} + \frac{\partial w}{\partial z}$$

The quantity $\nabla \cdot \mathbf{u}$ is also known as the **divergence** of the velocity field (notation often used is for divergence is $\text{div } \mathbf{u}$). In incompressible flow, velocity divergence is zero.

For flow past obstacles, we must consider a **boundary condition** on a wall. If the direction normal to the wall is \mathbf{n} , and the wall is moving with velocity \mathbf{U} , then for the fluid near the wall not to flow into the wall (if it could, that wouldn't be much of a wall, would it?), we must require that

$$\mathbf{u} \cdot \mathbf{n} = \mathbf{U} \cdot \mathbf{n}$$

Moreover, if the wall is stationary, the boundary condition becomes simply $\mathbf{u} \cdot \mathbf{n} = 0$. This is what is referred to as the **free-slip boundary condition**. In real life, flow is slowed near obstacles,

however, it is a manifestation of the same viscous dissipation that we chose to neglect when we decided that the flow is inviscid.

A special case of ideal flow is **potential flow** which is characterized by the existence of a function ϕ (velocity potential) such that the velocity field components (u, v, w) can be represented as

$$u = \frac{\partial \phi}{\partial x}, \quad v = \frac{\partial \phi}{\partial y}, \quad w = \frac{\partial \phi}{\partial z},$$

or, in vector notation, $\mathbf{u} = \nabla \phi$. In this case, the continuity equation becomes

$$\nabla^2 \phi = 0,$$

and it (with appropriate boundary conditions) can be solved for ϕ alone, without the momentum equation. After the solution for ϕ is obtained, the velocity components must be plugged into the momentum equation to solve for pressure p .

2. Theory of two-dimensional potential flows.

For the time being, let us consider **two-dimensional flow**. In reality, hydrodynamic phenomena default to being three-dimensional (3D) – any flow-related function of interest depends on spatial coordinates (x, y, z), although physically interesting flows where the z -dependence is weak or negligible can be found. So two-dimensional (2D) flow is a useful approximation (but one must always be aware that it is an approximation, and question the limits of its applicability to any real flow of interest). With these caveats, let us assume that

$$\frac{\partial}{\partial z} \ll \frac{\partial}{\partial x}, \frac{\partial}{\partial y}$$

With the z -derivative neglected, the continuity equation from (1.1) becomes

$$\frac{\partial u}{\partial x} + \frac{\partial v}{\partial y} = 0$$

Let the flow be **steady** ($\partial/\partial t = 0$, the flow pattern is time-independent). Further, let us assume that a velocity potential ϕ exists, so that

$$u = \frac{\partial \phi}{\partial x}, \quad v = \frac{\partial \phi}{\partial y},$$

Along with the potential ϕ , let us construct a **velocity streamfunction** ψ such that

$$u = \frac{\partial \psi}{\partial y}, \quad v = -\frac{\partial \psi}{\partial x} \tag{2.1}$$

For any ideal 2D flow, defining the velocity field also makes it possible to define the streamfunction. Consider two points in the flow separated by a small distance $\delta \mathbf{r}$. Let q be the volume flow rate (assuming that our 2D planar flow has unit depth in the out-of- x - y -plane direction) in the direction normal to $\delta \mathbf{r}$. Let $\delta \psi = q \delta r$. Then let $\delta r \rightarrow 0$ and rearrange the terms:

$$q = \frac{d\psi}{dr} \tag{2.2}$$

Now consider flow in a 2D plane with Cartesian coordinates (x, y). Let us assume that q is positive if, for an observer looking along an arbitrary axis in the direction of the flow, the flow appears crossing the axis from *left to right*. Selecting the x - and y -axis as the directions of observation then would produce (2.1). Also note the method of construction relating the streamfunction to the flow rate – we will use this feature later.

One notable feature of the streamfunction is that the 2D flow defined via its streamfunction satisfies the continuity equation from (1.1) by construction:

$$\frac{\partial^2 \psi}{\partial x \partial y} - \frac{\partial^2 \psi}{\partial y \partial x} = 0$$

For potential flow, this also means that the flow equations for the velocity field defined via (2.1) are satisfied automatically.

Now let us define an important quantity based on the velocity field: **vorticity**, which quantifies the amount of swirling (or shearing) motion in the flow. In the previous section, we defined divergence $\text{div } \mathbf{u} = \nabla \cdot \mathbf{u}$ using rules for a scalar product between the vectors ∇ and \mathbf{u} . Similarly, one can formally construct a vector product using the same quantities:

$$\boldsymbol{\omega} = \nabla \times \mathbf{u} = \det \begin{bmatrix} \mathbf{i} & \mathbf{j} & \mathbf{k} \\ \frac{\partial}{\partial x} & \frac{\partial}{\partial y} & \frac{\partial}{\partial z} \\ u & v & w \end{bmatrix} \quad (2.3)$$

Here $(\mathbf{i}, \mathbf{j}, \mathbf{k})$ is the triad of unit vectors in the (x, y, z) directions correspondingly. For the time being, let us consider the 2D case, when $w = 0$ and $\partial/\partial z = 0$. In that case, only one component of the vector product (in the z -direction) is non-zero:

$$\boldsymbol{\omega} = \mathbf{k} \left(\frac{\partial v}{\partial x} - \frac{\partial u}{\partial y} \right) = \mathbf{k} \omega$$

Next let us consider **irrotational 2D flow**: $\boldsymbol{\omega} = 0$. Using this condition of irrotationality together with the definition of the streamfunction, we obtain:

$$0 = \omega = \frac{\partial v}{\partial x} - \frac{\partial u}{\partial y} = \frac{\partial}{\partial x} \left(-\frac{\partial \psi}{\partial x} \right) - \frac{\partial}{\partial y} \left(\frac{\partial \psi}{\partial y} \right) = -\nabla^2 \psi$$

In other words, the streamfunction of the irrotational flow also satisfies the Laplace equation. Isocontours of the streamfunction (streamlines) have already been introduced in the preceding section of this course, moreover, using the same reasoning as we used to prove the streamfunction's existence, we can also prove that difference in the value of ψ between two streamlines equals the volume of fluid flowing between them. Additionally, the families of streamlines $\psi = \text{const}$ and of potential lines $\phi = \text{const}$ are orthogonal at every point in the flow.

3. Complex variable representation of 2D ideal flow.

Let us recall the Cauchy-Riemann condition for a function F of complex variable $z = x + iy$ to be holomorphic¹. If we write this function as a sum of its real and imaginary parts in Cartesian coordinates

$$F(z) = \phi(x, y) + i \psi(x, y), \quad (3.1)$$

the Cauchy-Riemann condition necessary for F to be holomorphic is

$$\frac{\partial \phi}{\partial x} = \frac{\partial \psi}{\partial y}, \quad \frac{\partial \phi}{\partial y} = -\frac{\partial \psi}{\partial x}$$

If we use potential ϕ as defined in Section 1 and streamfunction ψ as defined in Section 2 to construct F in (3.1), the Cauchy-Riemann condition will be satisfied automatically and, for differentiable ϕ and ψ , F will be a holomorphic complex variable function that defines the flow by defining the potential, the streamfunction, satisfying the Laplace equation for ϕ and ψ automatically, and being directly related to the flow velocity components (u, v) :

¹ Holomorphic - differentiable in a neighborhood of every point within its domain. From here on, we will assume that the reader is familiar with the fundamentals of complex-variable theory.

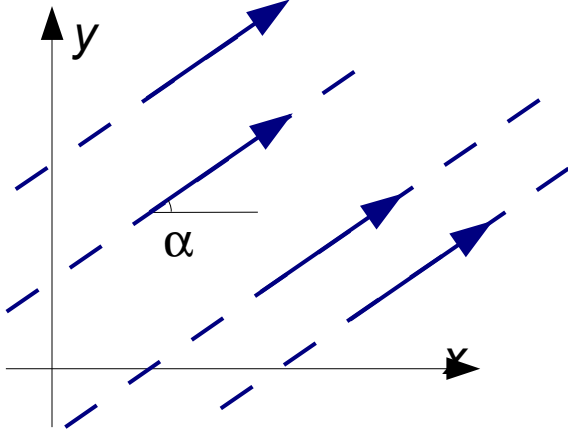
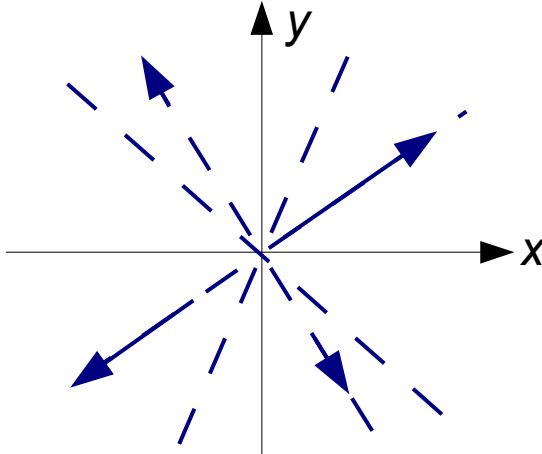
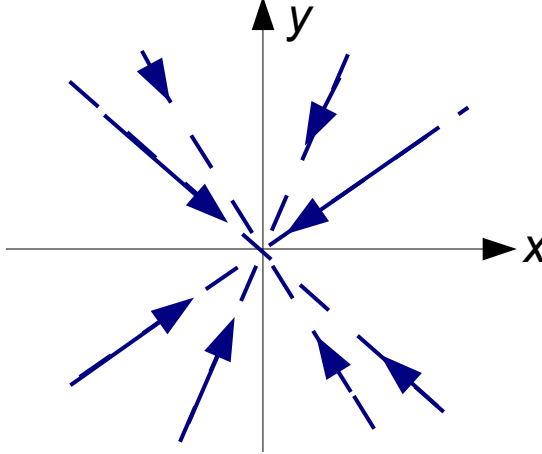
Description and schematic of the flow	Complex potential, velocity, etc.
<p>Uniform flow at angle α to x-axis</p> 	$F(z) = C e^{-i\alpha} z$ $w(z) = \frac{dF}{dz} = C e^{-i\alpha} = C \cos \alpha - i C \sin \alpha$ $u = C \cos \alpha, \quad v = C \sin \alpha$
<p>Point source at origin</p> 	$F(z) = C \log z = C \log(r e^{i\theta}) = C (\log r + i\theta)$ <p>C – real, positive</p> $\varphi = C \log r, \quad \psi = C \theta$ $w(z) = \frac{dF}{dz} = \frac{C}{z} = \frac{C}{r} e^{-i\theta}$ $u_r = \frac{C}{r}, \quad u_\theta = 0$ <p>Source strength (discharge rate)</p> $m = \int_0^{2\pi} u_r r d\theta = \int_0^{2\pi} C d\theta = 2\pi C$
<p>Point sink at origin</p> 	$F(z) = C \log z = C \log(r e^{i\theta}) = C (\log r + i\theta)$ <p>C – real, negative</p> $\varphi = C \log r, \quad \psi = C \theta$ $w(z) = \frac{dF}{dz} = \frac{C}{z} = \frac{C}{r} e^{-i\theta}$ $u_r = \frac{C}{r}, \quad u_\theta = 0$

Figure 1. Some common examples of ideal 2D flow and their representations with complex potential theory.

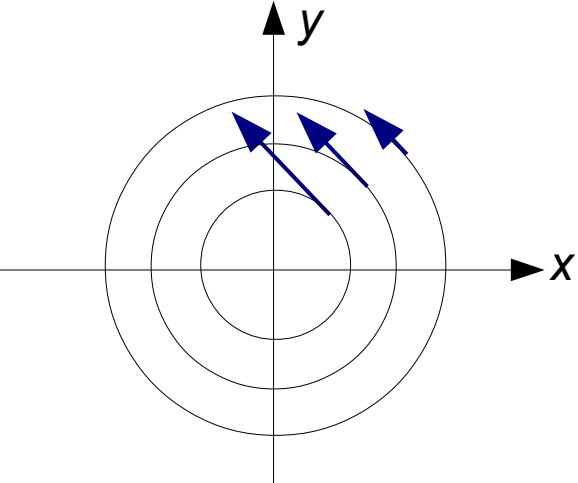
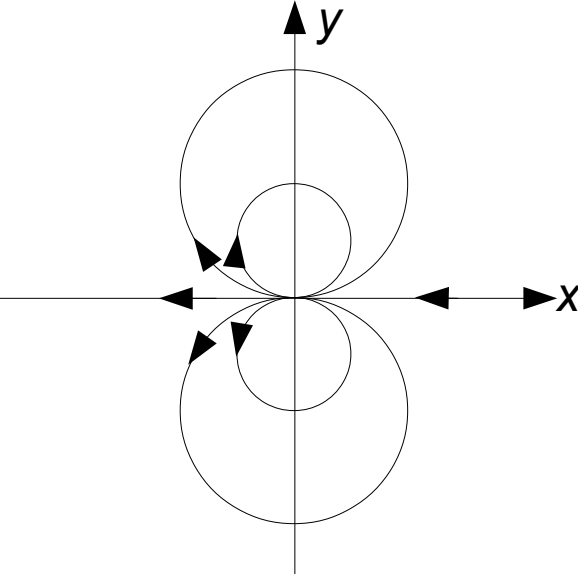
Description and schematic of the flow	Complex potential, velocity, etc.
<p>Point vortex at origin</p> 	$F(z) = -iC \log z = -iC \log(r e^{i\theta})$ $= -iC \log r + C \theta$ <p>C - real, positive</p> $\varphi = C \theta, \quad \psi = -C \log r$ $w(z) = \frac{dF}{dz} = -i \frac{C}{z} = -i \frac{C}{r} e^{-i\theta}$ $u_r = 0, \quad u_\theta = \frac{C}{r}$
<p>Doublet at origin</p> 	$F(z) = \frac{\mu}{z}$ <p>μ - real, positive (doublet strength)</p> $w(z) = -\frac{\mu}{z^2} = -\frac{\mu}{r^2} e^{-i\theta} (\cos \theta - i \sin \theta)$ $u_r = -\frac{\mu}{r^2} \cos \theta$ $u_\theta = -\frac{\mu}{r^2} \sin \theta$

Figure 1 (continued). Some common examples of ideal 2D flow and their representations with complex potential theory.

$$w = dF/dz = u - iv$$

Several useful flow fields can be constructed using some of the most common holomorphic functions (Fig. 1). While the construction of the flow fields for uniform flow, source, and sink is fairly obvious, the point vortex and the doublet deserve some discussion. In the discussion that follows, we will use both the Cartesian (x,y) and polar (r,θ) coordinates in the plane of the complex variable z .

First, in the case of the point vortex, at the center of rotation (origin) the complex potential reaches a **singularity**, and so does the complex velocity (with its radial component

undefined, and the tangential component going to infinity). Second, let us define **circulation** of the vortex along a closed contour L :

$$\Gamma = \oint_L \mathbf{u} \cdot d\mathbf{l}$$

Consider L as a circle with radius r and center at the origin (to make integration simpler). Then

$$\Gamma = \oint_L \mathbf{u} \cdot d\mathbf{l} = \int_0^{2\pi} u_\theta r d\theta = 2\pi C$$

Note that for all closed contours including the origin circulation Γ will remain the same.

Moreover, for any closed contour L' not including the origin,

$$\Gamma_{L'} = \oint_{L'} \mathbf{u} \cdot d\mathbf{l} \equiv 0$$

Now let us discuss the complex potential $F(z) = \mu/z$ that produces the doublet. Any streamline ($\psi = \psi_0$) can be proven to be a circle of radius $\mu/(2\psi_0)$ and center at $x = 0, y = -\mu/(2\psi_0)$. The formula for this potential can be derived by considering a source and a sink of equal strength at a small distance from each other, and letting this distance go to zero in a certain way.

There are other useful flow patterns described by complex variables. Moreover, combinations of complex potentials (e.g., a sum of two potentials) by constructions produce more complex potentials, some of which can also be useful. Similarly, translation of a complex potential likewise produces a potential, but any singularity the original potential has will move accordingly. Take, for example, a point vortex with circulation Γ at the origin, whose complex potential is $F(z) = -i\Gamma/(2\pi) \log z$. Based on this expression, the potential for a point vortex at $z = z_0$ would be $F(z) = -i\Gamma/(2\pi) \log z$. With the complex potentials at our disposal, we can now explore construction some potentials of greater complexity, ultimately leading us to the theory that allows to predict performance of lifting surfaces.

4. Ideal 2D flow past a cylinder.

Consider the sum of two potentials from the previous section (Fig. 1) – uniform flow ($\alpha = 0$) and flow past a doublet:

$$F(z) = Uz + \frac{\mu}{z}$$

The potential and streamfunction of the combined flow can be obtained by finding the real and imaginary parts of $F(z)$:

$$F(z) = Ure^{i\theta} + \frac{\mu}{re^{i\theta}} = \left(Ur + \frac{\mu}{r}\right) \cos \theta + i \left(Ur - \frac{\mu}{r}\right) \sin \theta$$

Thus the streamfunction is

$$\psi = \left(Ur - \frac{\mu}{r}\right) \sin \theta$$

Consider the streamline $\psi = 0$. It is easy to see that on this streamline, we must have $Ur - \mu/r = 0$, thus the streamline $\psi = 0$ is simply a circle of radius $a = (\mu/U)^{1/2}$. We can use this expression for a to rewrite the complex potential as

$$F(z) = U \left(z + \frac{a^2}{z} \right)$$

We can also consider two limit cases here. As $z \rightarrow \infty$, the term representing the uniform flow dominates, thus we have uniform flow at infinity. As $z \rightarrow 0$, the term representing the doublet becomes dominant, thus we have a doublet at the origin. Let us also remember that $\psi = 0$ is a

streamline. The combined flow pattern is shown in Fig. 2.

One feature of ideal flow as defined in Section 1 that we can take to our advantage is that the boundary condition on a solid surface is free-slip (velocity is parallel to the surface). Thus we can select any streamline as the solid-body boundary. For example, if we select the streamline $\psi = 0$ as the body boundary, then the flow field outside the circle $r = a$ in Fig. 2 will represent ideal 2D flow past a cylinder of radius a .

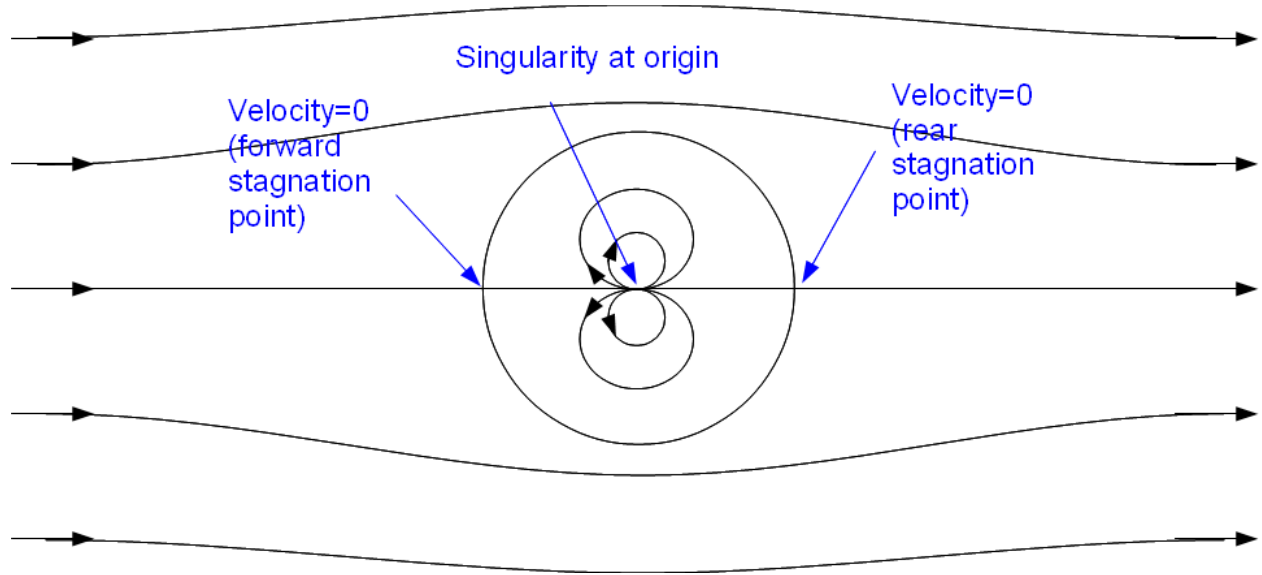


Figure 2. Ideal flow past a cylinder.

The flow field in Fig. 2 is characterized by a singularity (due to the doublet) at the origin. Let us also pay some attention to the pattern of streamlines. Almost everywhere in the field, there is only one streamline going through a given point (and a unique velocity). One exception to this rule is the singularity itself (but it would not be a part of our flow past the cylinder, as it would be inside of it). Two other exceptions are marked in the figure as forward and rear stagnation points. At stagnation points in the flow, velocity drops to zero, and streamline direction may be non-unique.

Further, we can add circulation to the flow by adding a point vortex at the origin to the complex potential:

$$F(z) = U \left(z + \frac{a^2}{z} \right) + \frac{i\Gamma}{2\pi} \log \frac{z}{a} \quad (4.1)$$

The z/a scaling results from adding a constant to $F(z)$ to keep $\psi = 0$ at $r = a$. The corresponding complex velocity is

$$w = \frac{dF}{dz} = U \left(1 - \frac{a^2}{z^2} \right) + \frac{i\Gamma}{2\pi} \frac{1}{z} \quad (4.2)$$

In polar coordinates,

$$w(z) = u - iv = (u_r - iu_\theta) e^{-i\theta}$$

For the velocity components in polar coordinates, we thus have

$$u_r = U \left(1 - \frac{a^2}{r^2} \right) \cos \theta, \quad u_\theta = -U \left(1 + \frac{a^2}{r^2} \right) \sin \theta - \frac{\Gamma}{2\pi r}$$

Now consider the velocity on the cylinder surface, $r = a$. For this case,

$$u_r = 0, \quad u_\theta = -2U \sin \theta - \frac{\Gamma}{2\pi a}$$

How does the addition of circulation Γ affect the location of the stagnation points? For stagnation points on the cylinder to exist on the cylinder surface, the tangential velocity component at $(r = a, \theta)$ must be zero as well, so

$$\sin \theta_s = -\frac{\Gamma}{4\pi U a}$$

Depending on Γ , a and U , this equation can have two, one, or zero solutions. In the latter case, while there are no stagnation points on the cylinder, they may exist elsewhere in the flow. Let us assume that a and U are fixed, and Γ is increased from zero. For small values of Γ , the flow pattern will resemble one shown in Fig. 2. Subsequent changes with Γ are illustrated in Fig. 3.

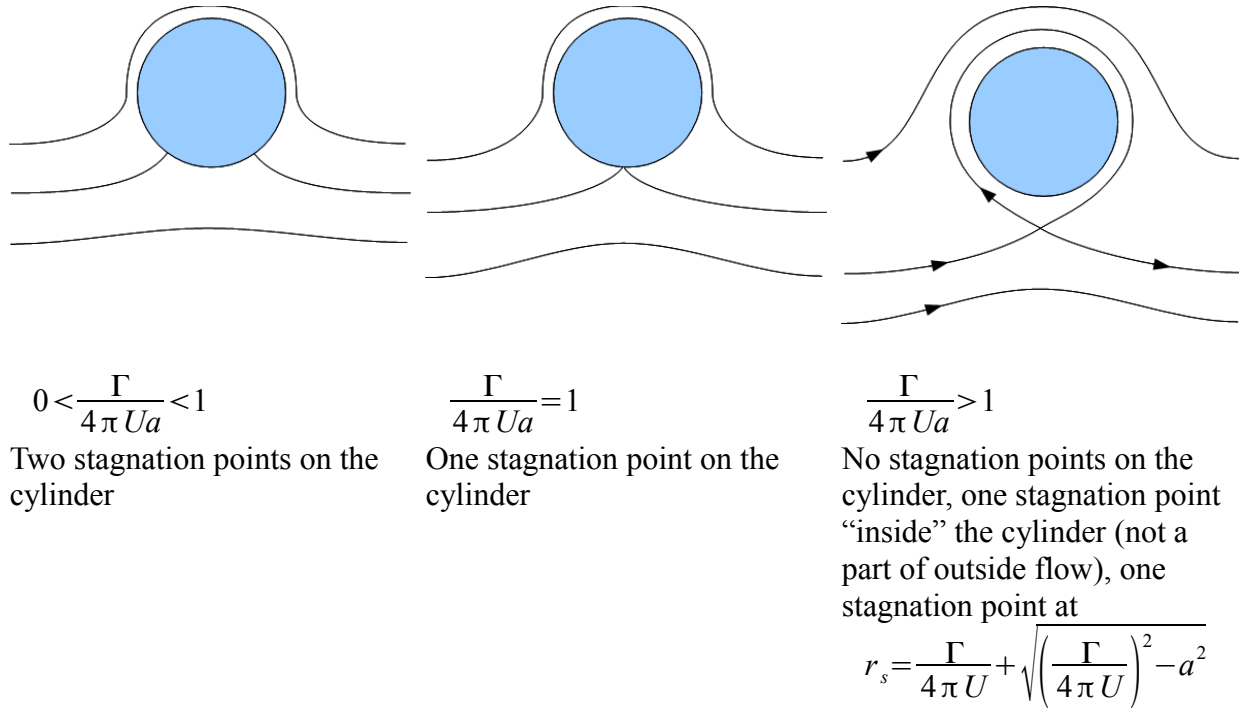
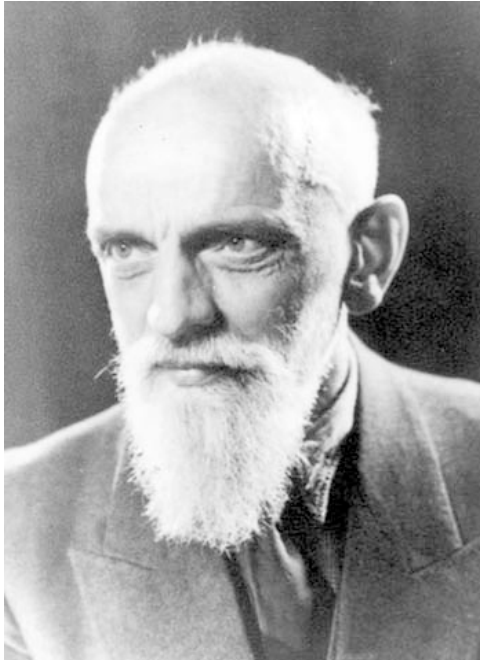


Figure 3. Stagnation points in flow past a cylinder with recirculation.

We will use this information about the effect of circulation on the stagnation points in cylinder flow later. Now, however, let us use complex variable theory to evaluate forces and moments on a body in fluid flow.

5. Forces and moments on a body in fluid flow, Blasius integral laws.

To find the force on a body in fluid flow in a general case, velocity components must be plugged into the momentum equation. The latter must then be solved to find pressure, and then the hydrodynamic force and moment can be found by appropriate integration over the body surface (in three dimensions) or contour (in two dimensions). Fortunately, in terms of complex potential for ideal 2D flows, the procedure is much simpler. Consider the complex force in the form



Paul Richard Heinrich Blasius

(1883-1970) in 1962.

"I tried to continue working in turbulence, again without success, and finally told myself: 'You are not a scientist.'"

$$X - iY,$$

where X and Y are the x- and y-components of the force acting upon the body due to the fluid flow around it.

Then let C_0 be an arbitrary contour fully enclosing the body. In 1910-1911, Blasius proved that both the fluid force and the moment M about the body's center of gravity can be evaluated as integrals along C_0 :

$$X - iY = i \frac{\rho}{2} \oint_{C_0} w^2 dz \quad (5.1)$$

$$M = \frac{\rho}{2} \operatorname{Re} \left(\oint_{C_0} z w^2 dz \right)$$

Here $w = dF/dz$ is the complex velocity. Both of these integrals, when evaluated in accordance with complex variable theory, can be easily resolved in terms of residues associated with singularities contained within the body contour.

As an example and for future use, let us apply Blasius first law (5.1) to the flow around a cylinder with circulation (4.1, 4.2):

$$w = \frac{dF}{dz} = U \left(1 - \frac{a^2}{z^2} \right) + \frac{i \Gamma}{2 \pi z}$$

Expression under the integral in (5.1) is

$$w^2 = U^2 - \frac{2U^2 a^2}{z^2} + \frac{U^2 a^4}{z^4} + \frac{i U \Gamma}{\pi z} - \frac{i U \Gamma a^2}{\pi z^3} - \frac{\Gamma^2}{4 \pi^2 z^2}$$

The sole singularity of w^2 is at $z = 0$. The integral can thus be trivially found with Cauchy's residue theorem:

$$X - iY = i \frac{\rho}{2} \oint_{C_0} w^2 dz = i \frac{\rho}{2} \left(2 i \pi \frac{i U \Gamma}{\pi} \right) = -i \rho U \Gamma$$

The results for the x-component of the force on the cylinder (referred to as **hydrodynamic drag**) and the y-component (hydrodynamic lift) are thus

$$\begin{aligned} X &= 0 && \text{(D'Alembert's paradox)} \\ Y &= \rho U \Gamma && \text{(Zhukovsky-Kutta law)} \end{aligned}$$

Zero drag result actually applies to *any body* in a non-separated steady ideal fluid flow. It is referred to as D'Alembert's paradox because in flows of real fluids, drag is non-zero. However, under the assumptions of ideal fluid theory, drag cannot be properly evaluated because one of the main mechanisms responsible for it (viscous dissipation) is explicitly disregarded. Later we will discuss how to deal with this problem, and how even in the context of viscous flow with drag, ideal-fluid theory still can be put to good use.

The result for the hydrodynamic moment of ideal flow around the cylinder can be similarly evaluated as $M = 0$. In the following sections, we will make good use of the result for lift we obtained in this chapter, but first we must develop mathematical apparatus that allows us to relate the flow around a lifting surface to the flow around the cylinder.

6. Conformal mapping and Zhukovsky transform.

Consider two planes of complex variables: $z = x+iy$ and $\zeta = \xi+i\eta$. Let us define a **conformal mapping** $\zeta = f(z)$, where f is a holomorphic function. Suppose we have a complicated contour in the z -plane that is reduced by a much simpler contour in the ζ -plane by this mapping (Fig. 4). The hope would be that, instead of solving for the flow in the z -plane, we could solve for it (with much simpler boundary conditions) in the ζ -plane, and then just remap the results to the original z -plane. Here we are helped by two features of conformal mapping. First, if in the (x,y) plane we have $\nabla^2\phi(x,y) = 0$, then in the (ξ,η) plane it will hold that $\nabla^2\phi(\xi,\eta) = 0$. In other words, conformal mapping preserves the Laplace equation. Second, we can show how complex velocities in the two planes are related:

$$w(z) = \frac{dF}{dz} = \frac{dF(\zeta)}{d\zeta} \frac{d\zeta}{dz} = \frac{d\zeta}{dz} w(\zeta)$$

Likewise, $w(\zeta) = dz/d\zeta w(z)$. Moreover, conformal mapping can be proven to preserve the strength of sources and sinks, as well as the circulation of vortices. Thus it is possible to use conformal mapping to greatly simplify the boundary conditions for the problems of ideal 2D hydrodynamics.



Nikolai Egorovich Zhukovsky
(1847-1921)

"Man will fly using the power of his intellect rather than the strength of his arms."

A variety of useful conformal mappings exists, but here we will use only one, named after N.E. Zhukovsky, who pioneered its use in lifting-surface studies in the late XIX and early XX century:

$$z = \zeta + \frac{c^2}{\zeta} \quad (6.1)$$

Let us note several properties of the Zhukovsky transform (6.1). First, as $|\zeta| \rightarrow \infty$, $\zeta \rightarrow z$, so the transform leaves the geometry of the far field (flow far away from the origin) the same in the z - and ζ -planes. Second, the velocity scaling factor for the Zhukovsky transform is easiest to express as

$$\frac{dz}{d\zeta} = 1 - \frac{c^2}{\zeta^2}$$

Note that in conformal mapping, the points where $dz/d\zeta = 0$ are called the **critical points** of the transform. Near such points, conformal mapping does not preserve the angle: a smooth curve passing through such a point in the ζ -plane will be mapped to a curve with a cusp in the z -plane. For Zhukovsky transform, the critical points are $\zeta = \pm c$.

Now let us begin the process of construction of the potentials for ideal steady flows past a variety of lifting surfaces in 2D. Our method for the construction of such flows will rely on using flow past a circular cylinder in the ζ -plane, then applying Zhukovsky transform (6.1) to map the cylinder to the contour of interest in the z -plane, then finding the appropriate flow pattern and the lift force on the body defined by that contour in the z -plane.

7. Ideal flow past a flat plate and the Zhukovsky-Chaplygin postulate.

Our procedure of constructing flows past lifting surfaces begins with a flow past a cylinder in the ζ -plane. Let us consider such a cylinder with radius c and a center at the origin. Thus both

critical points of the transform will be on the cylinder surface. From (4.1) with no circulation, the complex potential for this flow with a freestream velocity U would be

$$F(\zeta) = U \left(\zeta + \frac{c^2}{\zeta} \right)$$

Let us next consider a more general case, when the freestream velocity is at an angle α with the horizontal axis. For that, consider the original flow in a plane ζ' rotated with respect to the ζ plane, so that $\zeta' = \exp(-i\alpha)\zeta$. Then, if in the ζ' plane

$$F(\zeta') = U \left(\zeta' + \frac{c^2}{\zeta'} \right),$$

then in the ζ plane we will have

$$F(\zeta) = U \left(\zeta e^{-i\alpha} + \frac{c^2}{\zeta} e^{i\alpha} \right)$$

This cylinder flow will have stagnation points at $\zeta = \pm ae^{i\alpha}$. Let us refer to the polar coordinates in the ζ -plane as to (ρ, ν) to distinguish them from the polar coordinates in the z -plane². Now let us transition to the z -plane. What happens to the cylinder $\rho = c$? Let us consider its parametric representation $\rho = c \exp(i\nu)$ and plug it into the Zhukovsky transform equation (6.1):

$$z = ce^{i\nu} + \frac{c^2}{ce^{i\nu}} = c(e^{i\nu} + e^{-i\nu}) = 2c \cos \nu$$

As $-1 < \cos \nu < 1$, this equation represents a horizontal line segment in the z -plane, stretching from $-2c$ to $2c$ (Fig. 4). In effect, during the transform here, a round hole is cut out of the ζ -plane, and then stretched flat to close it in the z -plane, with the upward-facing side of the segment representing the upper half of the circle ($0 < \nu \leq \pi$) and the downward-facing side representing its lower half ($\pi < \nu \leq 2\pi$).

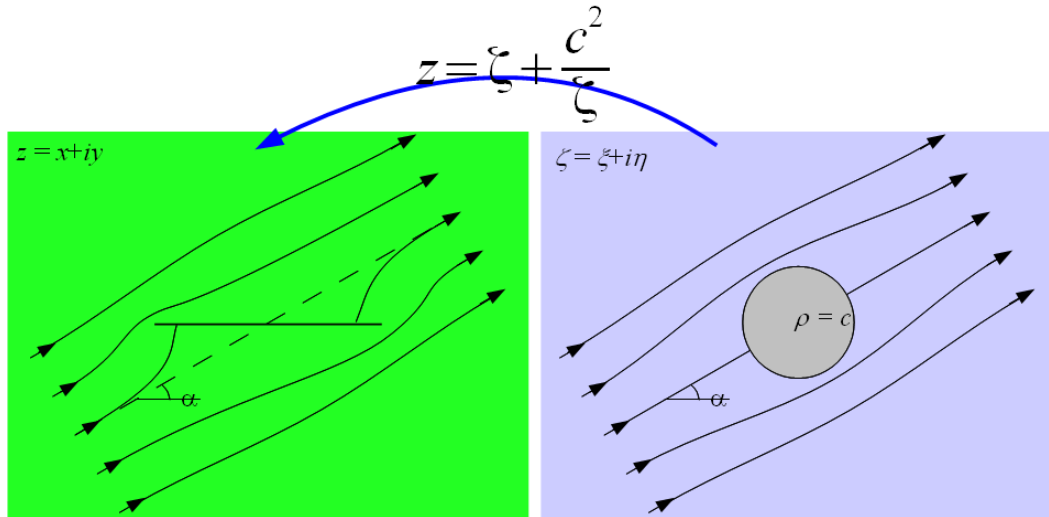


Figure 4. Zhukovsky transform producing flow at an angle of attack past a flat plate.

The flow pattern on the left panel of Fig. 4 resembles a real flow past a flat plate at an angle of attack, however, there are some important problems with this streamline pattern. Most notably, in realizable flows past flat plates and slender lifting surfaces with a defined trailing edge, the rear

2 Note that the Greek letters for polar coordinates in the z -plane are italicized to avoid confusion, because we already have non-italicized ρ denoting density.

stagnation point always is at the trailing edge (Fig. 5). It has to deal with the viscous dissipation in real fluid or gas bringing the velocity on approach to a stationary solid surface down to zero. Zero velocity condition on a solid boundary is known as the **no-slip boundary condition**. Sadly, in ideal fluid theory there is no way either to account for viscous dissipation or to satisfy this boundary condition with non-trivial flow. Another problem with sharp edges is that in ideal-fluid theory velocity of the flow around a sharp edge can become singular. This limitation could have proven fatal to any attempt to use ideal fluid theory to estimate lift produced by a wing. However, a cunning kludge was contrived by several researchers in the beginning of the XX century. It is referred to as the Kutta condition or (more accurately) the Zhukovsky-Chaplygin postulate.

The statement of the postulate is as follows:



Sergey Chaplygin
(1869-1942),
Hero of Socialist Labour
(1 February 1941)

“FOR BODIES WITH SHARP TRAILING EDGES AT MODEST ANGLES OF ATTACK TO THE FREESTREAM, THE REAR STAGNATION POINT WILL STAY AT THE TRAILING EDGE.”

This ensures that the velocity at the trailing edge is zero, and the streamline pattern is physically correct. Practically, to satisfy the postulate, one needs to add circulation to the flow in the ζ -plane to move the stagnation point in the z -plane to the trailing edge.

In the case of the flat plate, this trailing edge is at $z = 2c$, which would correspond to $\zeta = c$, while without circulation, the rear stagnation point in the flow past a cylinder at angle α to the horizontal axis resides at $z = ce^{i\alpha}$. From section 4, adding circulation Γ moves the stagnation point on the cylinder of radius a by an angle θ_s , so that

$$\sin \theta_s = -\frac{\Gamma}{4\pi U a}$$

By letting $a = c$ and $\sin \theta_s = -\sin \alpha$, we can select the right value of circulation to move the stagnation point to $\zeta = c$ (Fig. 5):

$$\Gamma = 4\pi U c \sin \alpha$$

Now we can use Blasius integral law (a.k.a. Zhukovsky-Kutta law, section 5) to relate lift Y on the plate to circulation (which, as section 6 mentions, should be preserved by the Zhukovsky transform). According to the Zhukovsky-Kutta law,

$$Y = \rho U \Gamma$$

Thus for the chosen value of Γ ,

$$Y = 4\pi \rho U^2 c \sin \alpha$$

This value represents the lift of a flat plate with length $4c$ and unit span (extent in direction normal to the x - y plane), and is in surprisingly good agreement with experiment for moderate velocities and angles of attack. Lift increases quadratically with U and nearly linearly with α (again, for modest angles of attack).

8. Lift coefficient.

Let us construct a dimensionless parameter characterizing lift on a slender wing. To do that, we must non-dimensionalize the lift force Y , using a physically relevant scaling factor constructed

from the dimensional parameters of the problem – U , ρ , l , where l is the characteristic length scale of the wing in the streamwise direction (Fig. 6). Note that this non-dimensionalization will work not just for wings, but (with appropriate modifications for geometry) for bluff bodies as well. For example, in defining the lift coefficient for a cylinder, the appropriate length scale would be its diameter.

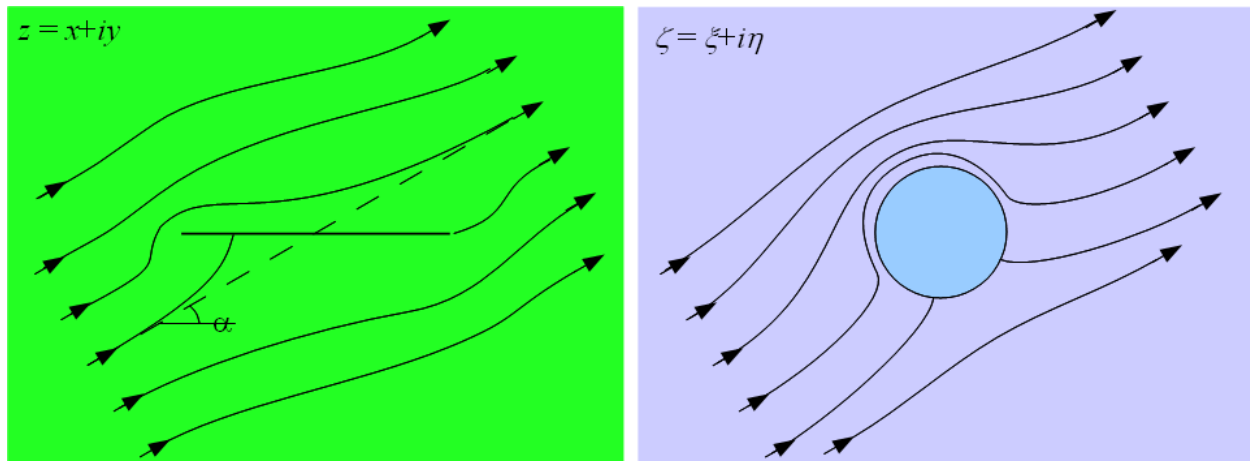
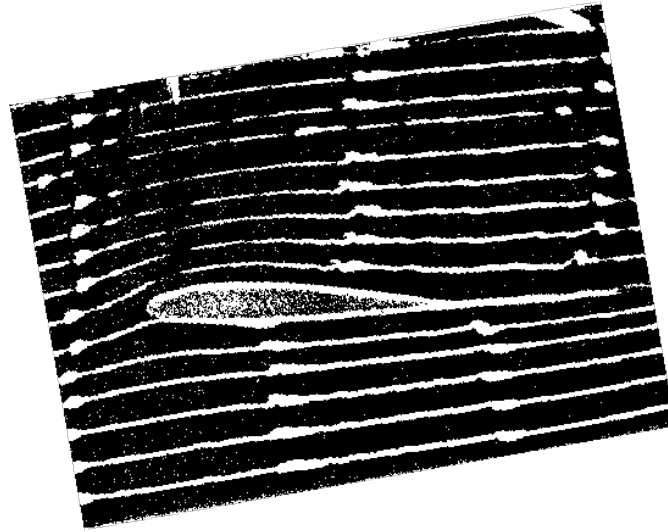


Figure 5. Top: smoke visualization of the flow past a lifting surface (image credit: Alexander Lippisch, 1953). Note the stagnation point on the trailing edge. Bottom: flat-plate flow with circulation added to satisfy the Zhukovsky-Chaplygin postulate.

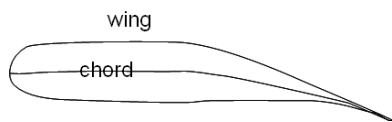


Figure 6. Chord – representative length scale of a lifting surface.

In terms of the chord length l , the lift coefficient for a lifting surface is then

$$C_L = \frac{Y}{\frac{1}{2} \rho U^2 l}$$

For the flat-plate flow we considered in the preceding

section, $l = 4c$ and

$$C_L = 2\pi \sin \alpha$$

Thus the lift coefficient increases with angle of attack. In real life, this phenomenon is

complicated with viscous effects. As the result, at some critical angle of attack, the flow on the upper surface of the wing will separate, creating a large zone of recirculating flow, leading to decrease of lift coefficient – condition known as stall. At modest velocities, the stall angle is typically about 15° . Flow separation can be controlled by variable wing geometry (for example, spoilers).

9. Wing with a Zhukovsky profile.

Section 7 provides us with an example of constructing a flow past a lifting surface using Zhukovsky transform applied to cylinder flow in the ζ -plane. By varying the size and position of the cylinder with respect to critical points of the transform ($\zeta = \pm c$), we can produce a variety of lifting-surface profiles. To create a sharp leading (or trailing) edge, one must position the cylinder to place the appropriate critical point on its surface.

Consider, for example, a profile with a smooth leading edge and sharp trailing edge (a symmetrical Zhukovsky airfoil, Fig. 7, top). To produce such a profile, the center of the cylinder in the ζ -plane has to be shifted left from the origin by a distance m . Let $m = \epsilon c$, where ϵ is small, and let us choose the radius of the cylinder so that the critical point $\zeta = c$ is on the surface of the cylinder: $r = a = c(1+\epsilon)$. The leading edge of the cylinder will then reside at $\zeta = -(c+2m)$. With linearization (neglecting quantities on the order of ϵ^2 and smaller), the chord length of the lifting surface in the z -plane corresponding to this cylinder is $4c$, and the maximum thickness t of the profile, occurring at $z = -c$, is

$$t = 3\sqrt{3} c \epsilon$$

The ratio between t and chord length l is called the **thickness ratio** of the wing. For the case of symmetrical Zhukovsky airfoil,

$$\frac{t}{l} = \frac{3\sqrt{3}}{4} \epsilon$$

Now consider the flow past this cylinder at an angle of attack α . The rear trailing edge of the wing in the z -plane is at $z = 2c$, corresponding to $\zeta = c$. Thus we want to move our stagnation point in the ζ -plane there, which means (similarly to the reasoning of Section 7) that we have to add circulation $\Gamma = 4\pi a U \sin \alpha$. Note that the cylinder radius for this case is

$$a = c + m = c(1 + \epsilon) \approx \frac{l}{4} \left(1 + \frac{4}{3\sqrt{3}} \frac{t}{l} \right) \approx \frac{l}{4} \left(1 + 0.77 \frac{t}{l} \right)$$

To satisfy the Zhukovsky-Chaplygin postulate, we need to add circulation

$$\Gamma = 4\pi U a \sin \alpha = \pi U l \left(1 + \frac{4}{3\sqrt{3}} \frac{t}{l} \right) \sin \alpha$$

As $t/l \rightarrow 0$, this expression is reduced to the expression for the flat plate. However, for small but non-zero thickness ratio, the amount of circulation is greater than that for the flat plate. The lift coefficient for the case of a symmetrical Zhukovsky airfoil is

$$C_L \approx 2\pi \left(1 + 0.77 \frac{t}{l} \right) \sin \alpha$$

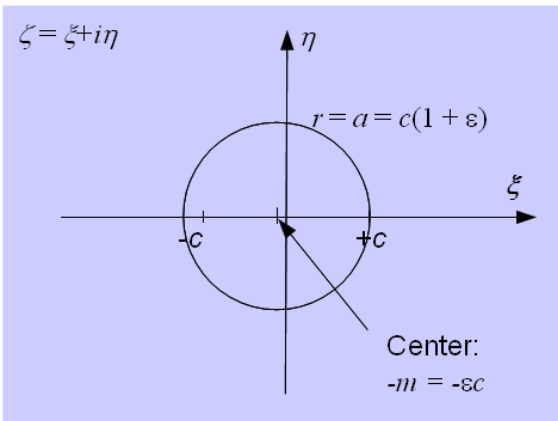
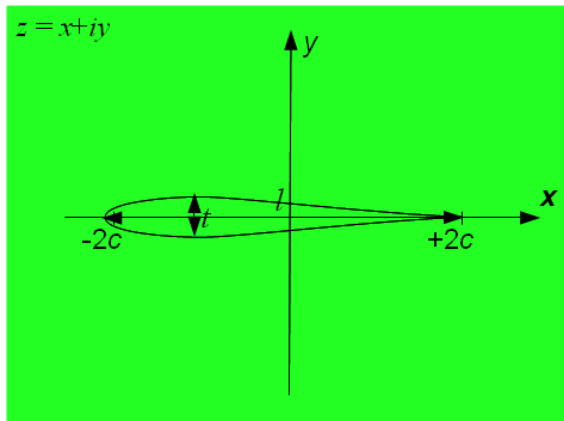
In other words, symmetrical Zhukovsky airfoil has better lift than the flat plate with the same chord length. Similarly, one can demonstrate that an arc-shaped airfoil with **camber** (arc height) h (Fig. 7, second row) also has better lift than the flat plate:

$$C_L = 2\pi U c \sin \left(\alpha + 2 \frac{h}{l} \right)$$

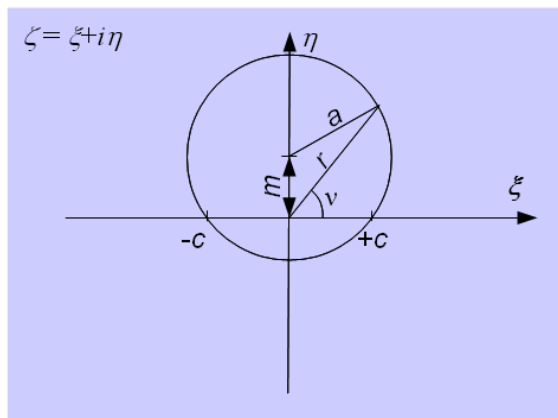
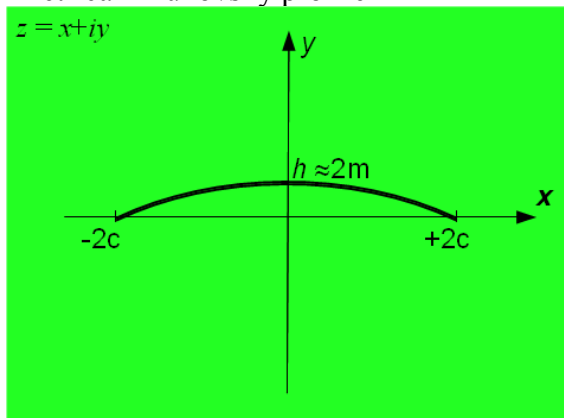
Then, to optimize lift, a surface with both thickness and camber (a general Zhukovsky profile) can be constructed, for which the lift coefficient will be

$$C_L = 2\pi \left(1 + 0.77 \frac{t}{l} \right) \sin \left(\alpha + \frac{2h}{l} \right)$$

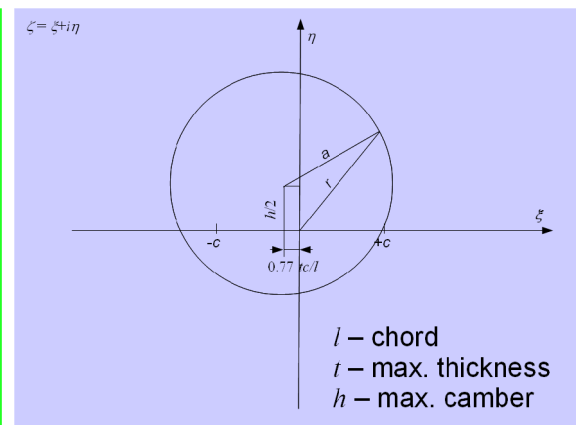
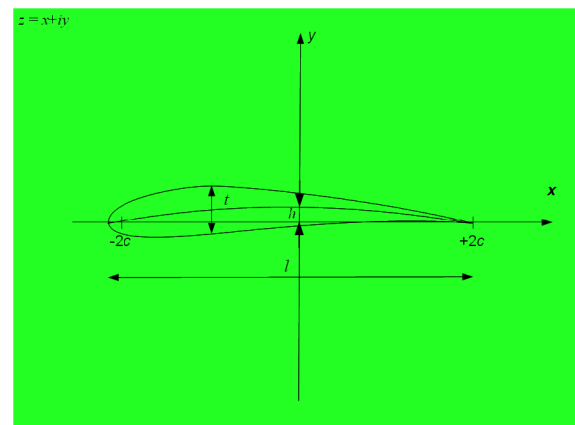
Many practical subsonic wing profiles closely resemble the general Zhukovsky profile.



Symmetrical Zhukovsky profile



Arc airfoil



Zhukovsky profile

Figure 7. Construction of lifting surfaces: top – symmetrical Zhukovsky profile, middle row – arc airfoil, bottom – general Zhukovsky profile.

10. Dealing with drag.

The methods described above help predict lift, but by construction cannot do anything about the drag force. To deal with the drag force, one needs to consider viscous flow, which has governing equations that are much more complicated than ideal flow: as viscous dissipation takes place, the energy equation has to be considered. That introduces additional variables, such as internal energy and temperature, and requires additional equations (for example, equations of state) and/or assumptions (for example, Newtonian viscosity) to close the system. One of the most common models of viscous flow is known as the Navier-Stokes equations. For incompressible flow,

A very useful simplification of the Navier-Stokes equations is the boundary layer approximation. Under this approximation, the flow outside the immediate vicinity of a solid surface is considered as inviscid, while the consideration of the viscous flow in the narrow zone near the surface uses simplifying assumptions based on order-of-magnitude analysis to disregard some terms, thus avoiding solving the full Navier-Stokes equations. Further, in the boundary layer, the exact functional forms of the solutions of the boundary layer equations can be replaced with polynomial representations (the Pohlhausen – von Karman method). Then the conservation equations for mass, momentum, etc. can be solved together with the boundary conditions to find the extent of the boundary layer and the polynomial coefficients. At the edge of the boundary layer, the boundary layer solution has to be asymptotically matched with the inviscid outer flow solution.

11. Experimental measurements of lift and drag.

In laboratory, lift and drag on a model of a lifting surface can be measured with an aerodynamic scale. In addition, flow visualization helps understand to what extent the ideal-flow patterns relate to the actual flow field.

12. Modeling lifting-surface flow with Xfoil.

Xfoil is a package written primarily by Professor Mark Drela (MIT) for analysis and design of subsonic isolated airfoils. The original version was released in 1986. It can perform both inviscid and viscous flow modeling.

For the inviscid analysis, the airfoil is modeled with a linear-vorticity streamfunction panel method. The airfoil surface is divided into piecewise straight line segments or panels or “boundary elements,” and vortex sheets of strength γ are placed on each panel. Think of a vortex sheet as of a line with a vortex at every point. The circulation a segment ds of the line thus imposes on the flow is $d\gamma$. By generating circulation (and thus lift) along the contour of the lifting surface, vortex sheets mimic the effect of the boundary layer around airfoils. In the latter, viscous effects produce shear along the surface, and shear leads to vorticity (and thus circulation) deposition in the flow.

For viscous modeling, the flow is separated into three zones (outer flow, boundary layer, wake). The outer flow is considered as inviscid. Profiles of variables in the boundary layer are approximated with an integral method.

We will not use all the features of Xfoil, but use it to predict lift and drag on lifting surfaces under conditions close to those we will realize in laboratory experiment. Xfoil is command-line driven, and versions for all modern operating systems exist. Let us start here with an assumption that you have either downloaded and installed an archive with appropriate Xfoil

binaries (on a Windows-based machine, the default directory for the installation would be `c:\xfoil`), or successfully compiled Xfoil from the source files on your system. The following narrative will use Windows environment for an example, mostly because a typical Windows user is in the greatest need of guidance.

Start with opening a command-line window (`Win + R`, then type `cmd` in the “Run” window that pops up). This should bring up a window. Stretch it out a little bit with the cursor, so that you should be able to see about fifty lines of text, change directory to the directory where the `xfoil.exe` file resides, then start xfoil:

```
cd \xfoil\bin
xfoil
```

The Xfoil summary (including the list of submenus) should display, and the command prompt should change to something like

```
XFOIL  c>
```

Now let us load a wing profile by typing

```
NACA 2412
```

Note that the NACA four-digit designator defines the wing profile by:

1. First digit describing maximum camber as percentage of the chord.
2. Second digit describing the distance of maximum camber from the airfoil leading edge in tens of percent of the chord.
3. Last two digits describing maximum thickness of the airfoil as percent of the chord.

The NACA 2412 airfoil that we loaded has a maximum camber of 2% located 40% (0.4 chords) from the leading edge with a maximum thickness of 12% of the chord. Four-digit series airfoils by default have maximum thickness at 30% of the chord (0.3 chords) from the leading edge.

Xfoil should respond by confirming some basic information about the wing (thickness, camber, etc.). Just in case, it's nice to force cleanup of the geometry as loaded:

```
pane
```

Then let us move to the `OPER` submenu to perform some operations (commands are not case-sensitive).

```
OPER
```

The prompt should change to

```
.OPERi c>
```

Note the “i” after “`OPER`” - this means that you are in inviscid mode. Now let us specify the angle of attack for which we need to perform the calculations:

```
alfa 0
```

This should bring up a window showing velocity and pressure distributions on the wing surface for the inviscid case. The lift coefficient C_L is also displayed. Please note that Xfoil assumes that the chord length of the profile is unity (thus the results may need rescaling to be compared with theory or experiment). Now let's switch to viscous flow by typing

```
visc
```

In response, xfoil will prompt you for the Reynolds number. Let's set it to

```
3e5
```

Let us redo the calculations for the viscous case:

* Windows key. In this narrative, text blocks with gray highlights denote keyboard keys or shortcut combinations, and text in `Courier` font shows interaction with the computer.

alfa 0

Along with the lift coefficient, the output window will now display the drag coefficient C_D (Fig. x). Also note that the inviscid results for velocity and pressure on the wing are also displayed for comparison, with dashed lines. In the bottom of the display window, the program will show the boundary layer and wake areas. Despite the very crude assumptions of the inviscid model, its prediction for the lift coefficient (0.255) turns out to be very close to the prediction of the model taking into consideration the viscous effects (0.235), and to the experiment as well. However, drag coefficient in this case cannot be predicted with ideal theory.

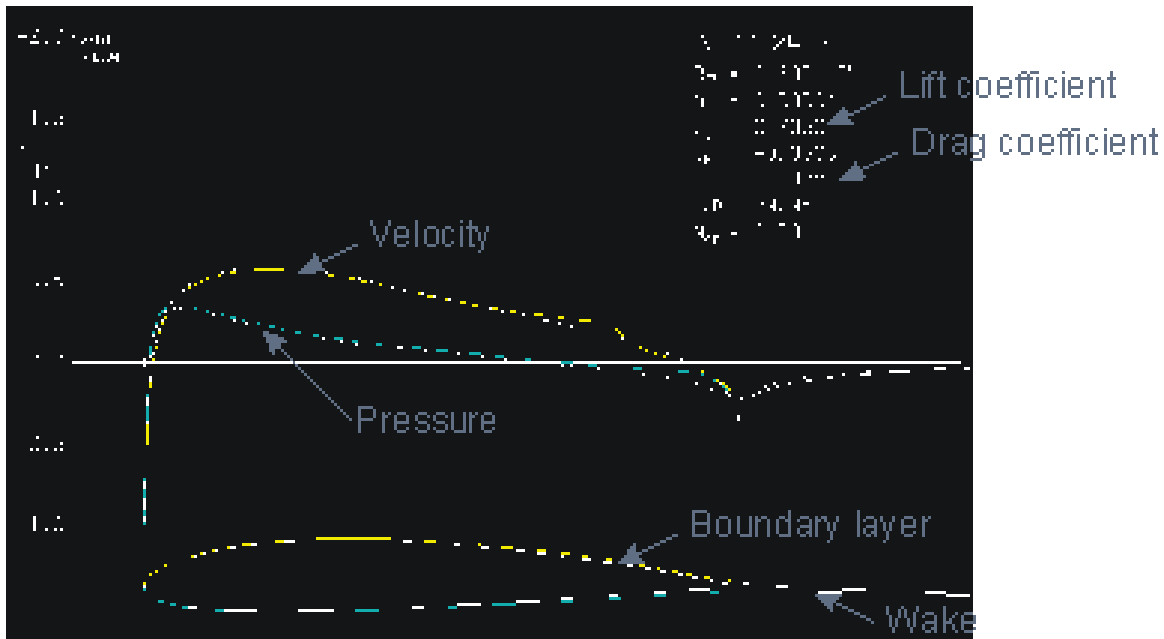


Figure x. Xfoil display output with features of interest labeled.